PCCP

PAPER

View Article Online
View Journal | View Issue

Cite this: *Phys. Chem. Chem. Phys.*, 2022, **24**, 15135

Observation of photoassociation spectroscopy of ^{23}Na spinor Bose–Einstein condensate

Wenliang Liu,[ab] Ningxuan Zheng,[a] Vladimir Sovkov,[ac] Jing Xu,[a] Yuqing Li,[ab] Yongming Fu,[a] Peng Li,[a] Jizhou Wu,*[ab] Jie Ma,*[ab] Liantuan Xiao[ab] and Suotang Jia[ab]

Received 17th February 2022,
Accepted 20th May 2022

DOI: 10.1039/d2cp00800a

rsc.li/pccp

We report the high-resolution photoassociation (PA) spectroscopy of ^{23}Na excited from the spin-1 Bose–Einstein Condensate (BEC) to the molecular state of $0_g^-(P_{3/2})v = 4$ and $1_g(P_{3/2})v = 91$. By comparing the PA spectra of different spin configurations, we experimentally studied the effect of spin on the PA spectra. The experimental spectra comply well with the theoretical consideration. The results will play an important role in the study of the spin interaction and control of the antiferromagnetism in Na.

1 Introduction

Bose–Einstein condensates (BECs) of atomic gases are universal and effective systems for observing various microscopic quantum effects.12 An important development direction of BEC research is the multi-component and multi-species quantum systems, which in part, can provide a unique opportunity to explore coupling, quantum coherence, and interaction of constituent spin components.[3–8] As representative multi-component quantum systems, spinor BECs have provided an exciting way to study spin-squeezing,[9] quantum magnetism,[10] quantum entanglement,[11] superfluidity,[12] and strong correlations.[13] In addition, the extended research of multi-component systems such as the demonstration of spontaneous breaking of spatial and spin symmetries,[14] the demonstration of skyrmions,[15] and studies of a quantum phase transition[16] are also very fascinating.

A spin-1 condensate is composed of three spin components of $m_F = -1$, 0, +1 states, corresponding to its three magnetic Zeeman sublevels. The interaction between the different internal components causes ferromagnetism or anti-ferromagnetism[17] in these systems. The spin-1 BEC of ^{23}Na was found to be anti-ferromagnetic,[18] while the ^{87}Rb system was predicted to be ferromagnetic.[19] This reflects differences in their ground state structure and dynamical properties. The atomic interactions and magnetic properties are dominated by two-body s-wave collisions and spin-dependent interactions in a spinor condensate.[20,21] Through a magnetic[22–24] or optical[25–27] Feshbach resonance, we can change the s-wave scattering length to achieve the purpose of control over the magnetic properties. Two advantages led us to use the optical Feshbach resonance. One is the optical coupling can be quickly turned on and off, and the other is that the optical Feshbach resonance can be applied to systems that do not have a convenient magnetic resonance available,[28] such as in the case of a large magnetic field of ^{23}Na.[29]

In the BEC photoassociation (PA) study, one more point must be mentioned. The extremely low temperature and high-density conditions in BEC indicate that we can achieve a high PA rate in experiments. PA can be used to measure and operate the scattering length, the magnetic properties of the system, and the interaction of spin components. Therefore, the research of the PA spectra of a spin-1 BEC is very important. Note that although there have been many studies on Na PA spectra,[30–33] no spinor and spin-dependent spectra have been reported.

In this paper, we report the high-resolution experimental PA spectroscopy of the spin-1 BEC of ^{23}Na. A series of PA spectra for different spin states was observed. A simple theoretical consideration to interpret spin spectra has been presented. This lays the foundation for further study of spin interactions and antiferromagnetic properties in BECs.

2 Experimental setup

The most basic and important step is to prepare the spinor BEC. The spin-1 BEC is achieved by performing experiments in an ultrahigh vacuum (UHV) chamber, in which the pressure is on the order of 10^{-11} mbar. Hot atoms are slowed down by the Zeeman slower[34] and then collected by the magneto-optical trap (MOT), which is composed of six beams and a pair of anti-Helmholtz coils. The magnetic field gradient along the *z*-axis is produced by the anti-Helmholtz coils. The MOT beams are

[a] *State Key Laboratory of Quantum Optics and Quantum Optics Devices, Institute of Laser Spectroscopy, Shanxi University, Taiyuan, 030006, China. E-mail: wujz@sxu.edu.cn, mj@sxu.edu.cn*
[b] *Collaborative Innovation Center of Extreme Optics, Shanxi University, Taiyuan 030006, China*
[c] *St. Petersburg State University, 7/9 Universitetskaya nab., St. Petersburg 199034, Russia*

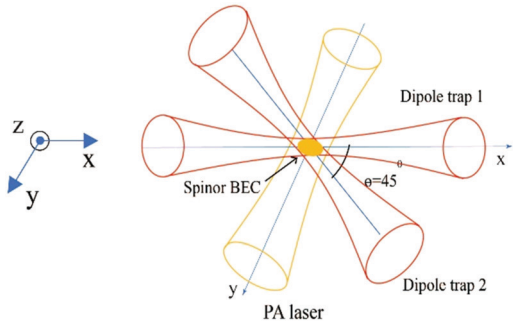

Fig. 1 Schematic view of the main experiment system. The spinor BEC is trapped in a crossed dipole trap (red beams). The crossed-beam dipole trap is also used for evaporative cooling. The focused PA beam is shown in an orange beam.

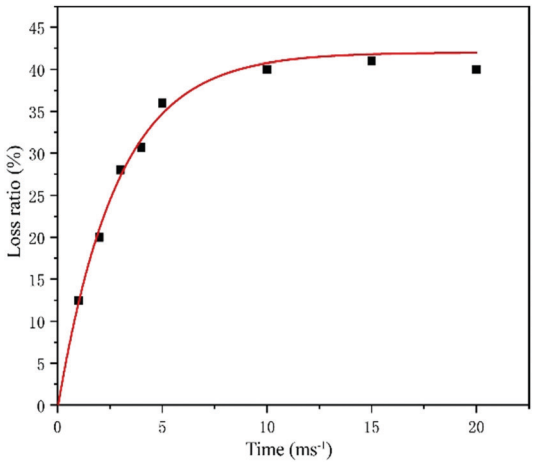

Fig. 3 The dependence of the maximum condensate loss on the PA pulse time for the intensity of 0.1 kW cm^{-2}.

supported by cooling beams and repumping beams. The cooling beams are detuned by $\delta_{\text{cooling}} = -20$ MHz from the ^{23}Na $|F = 2\rangle \rightarrow |F = 3\rangle$ transition and the repumping beams are detuned by $\delta_{\text{repump}} = -5$ MHz from the ^{23}Na $|F = 1\rangle \rightarrow |F = 2\rangle$ transition, as shown in Fig. 2(b). After 8 s of MOT loading, we typically capture above 5×10^9 atoms with a temperature of about 350 μK. In order to further reduce the temperature, we took the steps of a compressed magneto-optical trap (CMOT) and molasses.[35] The specific details of the experimental sequence are shown in Fig. 2(a). These two processes efficiently cool 1.7×10^8 atoms to 45 μK. The repumping beams are closed 1 ms earlier than cooling beams. The purpose is to depump atoms into the $F = 1$ hyperfine states and load atoms to the dipole trap.

We employed a crossed dipole trap to collect and evaporate the cooled atoms. A single-mode fiber amplified laser (1070 nm, IPG FLR-100-LP) was used to provide large-detuned and high intensity beams. The dipole trap is formed by two focusses intersecting beams on the horizontal X–Y plane. As shown in Fig. 1, both beams are focused to a $1/e^2$ beam diameter of 32 μm (38 μm) and power of 13 W (14 W) in the $X(Y)$ direction. The trapping frequencies of the dipole trap measured by the parametric heating method are 2.7, 2.8 and 5 kHz corresponding to the X, Y and Z directions. At the beginning of the experiment, the dipole beams were turned on at half power. After the molasses process, the power of the dipole beams immediately rises to full and holds for 500 ms. This method can greatly increase the loading rate of atoms.[36] There are 6×10^6 atoms trapped in the dipole trap. The forced evaporation cooling is executed by reducing the potential of the dipole trap, that is, the power of the dipole beams. The potential is exponentially reduced in 3 s. After 3 s of forced evaporative cooling, we observe spinor Bose–Einstein condensation with an atom number of 5×10^5 and phase space density of 8.3. At this point, the three spin components are degenerated and in the $F = 1$ state.

Fig. 2(c) shows the schematic diagram of the Na_2 potentials. After a condensate is formed, a PA laser is used to couple colliding atoms to excited molecular levels, which are subsequently lost from the trap. The excited molecule decays into either a stable molecule or a pair of energetic free atoms (shown by the dashed arrows in Fig. 2(c)). This results in a loss of atoms from the trap. The spectrum of the molecular excited states is measured by monitoring the loss of the atom number under different frequencies of the PA beam. The number of atoms left in the trap after the action of the PA pulse is measured by the absorption images. The PA laser has a focused waist radius of 62 μm and an intensity of 50 W cm^{-2}. The frequency of the PA laser is locked by a wavelength-meter feedback system. Frequency stability accuracy is about 6 MHz. As shown in Fig. 3, we

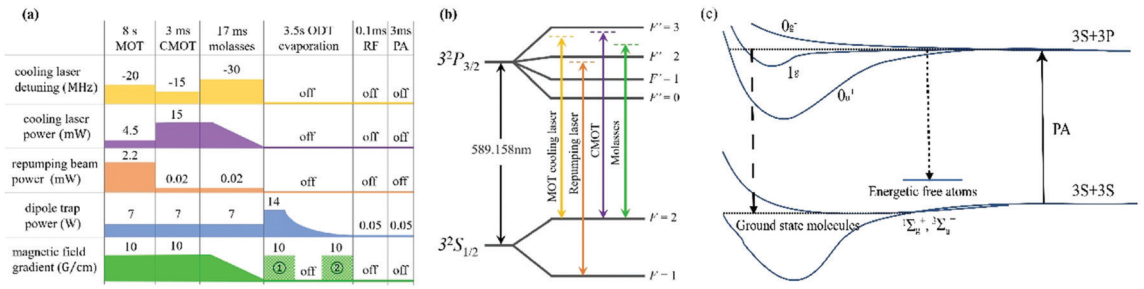

Fig. 2 (a) Experimental sequence of creating sodium BECs with the all-optical approach (see text). (b) The diagram of transitions in a typical experimental sequence for our all-optical BEC approach. (c) Schematic diagram of the Na_2 potentials showing mechanisms for photoassociation, and trap loss. The solid arrows show a PA process. The dashed arrows show how the excited molecules might decay into ground state molecules and energetic free atoms, respectively.

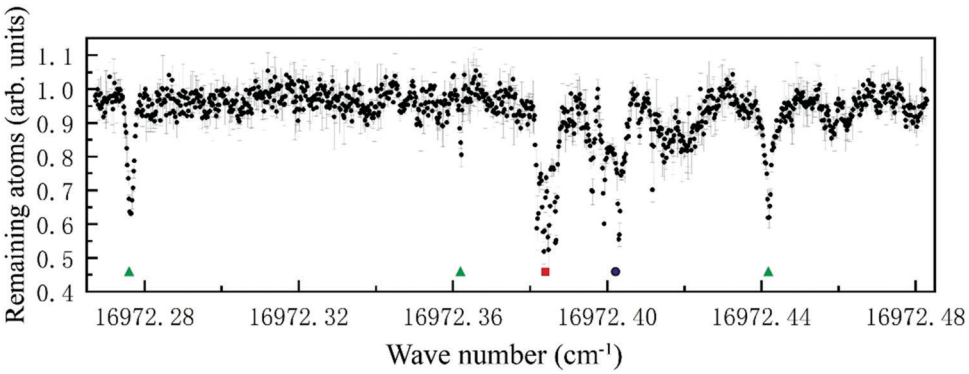

Fig. 4 The experimental ^{23}Na PA spectrum of the excited molecular state. This spectrum is obtained by applying the PA beam with the intensity of 50 W cm^{-2} and the waist radius of 62 μm on the condensates for 10 ms. The interval between adjacent data points is 6 MHz. The resonances of 0_u^+ are indicated by the green triangles. They are v = 36 to v = 38 from left to right. The transition to the 0_g^- (v = 4) is indicated by the red square. The blue circle indicated the state of 1_g (v = 91).

measured the saturation effect of the spectrum. The frequency of the PA laser is 16972.4378 cm^{-1}. The PA light pulse reaches saturation around 10 ms. A PA pulse with a duration of 10 ms is used to couple the atoms. The PA laser is locked once every 6 MHz and three experiments are performed for each lock. The total number of atoms in the condensate measured by three experiments is counted and normalized to the average value. For each experiment, the absorption imaging was performed 3 ms after the PA light and dipole light had been turned off. One of the registered spectra is shown in Fig. 4.

In order to explore the influence of different spin states on the PA spectrum, we prepared different spin components. To create a pure $m_F = -1$ state, we apply a 10 G cm^{-1} gradient field within 1 s at the start of forced evaporation (as shown in shaded area ① in Fig. 2(a)).[36] To create a pure $m_F = 0$ state, we apply a 20 G cm^{-1} gradient field within 1 s at the end of forced evaporation (as shown in the shaded area ② in Fig. 2(a)).[37] For the pure $m_F = +1$ state, we need to use radio frequency (RF) to transform from an $m_F = -1$ state. By adjusting the frequency and amplitude of the radio-frequency signal, we can transfer the condensates in the $m_F = -1$ to $m_F = +1$ or into a mix of $m_F = 0, \pm 1$. (The proportions of the two spin states are not equal. There are about 20% more atoms in the +1 state than in the 0 state.) For the mixed $m_F = 0, -1$ state, we apply a gradient field of about 20 G cm^{-1} within 300 ms at the start of forced evaporation. The $m_F + 1$ state is the high-field-seeking-state. These atoms escape the trap during this 300 ms evaporation. For the mixed $m_F = +1, -1$ state, we first prepare all atoms to the $m_F = 0$ state. After adjusting the frequency of RF, the mixed $m_F = +1, -1$ state can be obtained.[37]

Fig. 5 shows the PA spectra of different spin components. We selected the range from 16972.36 cm^{-1} to 16972.39 cm^{-1} as the one with rich spectral lines. We first observe the spectrum of the non-polarized $F = 1$ ensemble shown in Fig. 5(a). The following Fig. 5(b)–(d) are the photoassociation spectra for different spin components.

The most striking difference of the three PA spectra is that the lines $F_{mol} = 0$ appear only for the condensate containing the $m_F = 0$ spin state. Obviously,[38] the two-body s-wave is only able

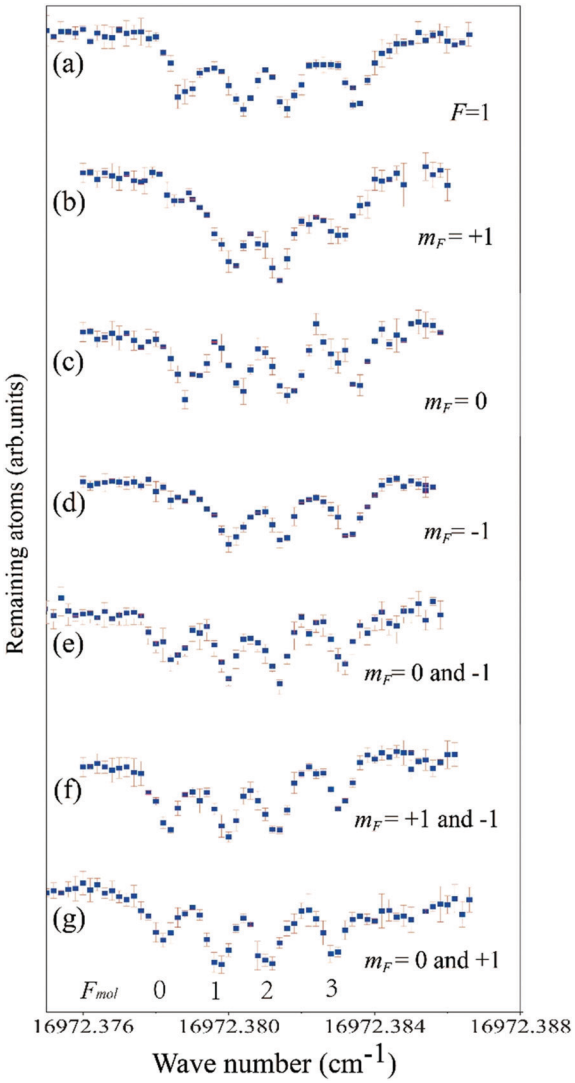

Fig. 5 The PA spectra of 0_g^- v = 4 for different spin components: (a–g) are the spectra of different spin components, F_{mol} designates the rotational structure. The parameters and action time of the PA light are the same as described in the caption of Fig. 4. The interval between adjacent data points is 6 MHz.

to form a molecular $F_{mol} = 0$ state in the channel with the zero total spin. The zero-total-spin channel is achieved in collisions of two $m_F = 0$ atoms or of the ones with the mutually opposite spin projections, *i.e.*, of $m_F = 1$ and $m_F = -1$, while the components $m_F = +1$ alone or $m_F = -1$ alone contribute to the molecular states with $F_{mol} \geq 2$. Taking into account the propensity rule $\Delta F_{mol} = 0, \pm 1$ of the electric dipole transition, the $F_{mol} = 0$ line can only be observed in PA of the condensate containing $m_F = 0$ or the mix of both $m_F = 1$ and $m_F = -1$, while pure $m_F = 1$ or $m_F = -1$ condensates cannot produce the $F_{mol} = 0$ lines.

To illustrate these predictions, the PA spectra across the lines $F_{mol} = 0$ are taken with condensates containing different mixtures of spin states as shown in Fig. 5(e)–(g). The observed data in Fig. 5(f) show that the $m_F = -1$ and $m_F = 1$ spin states participate in the photoassociation to the $F_{mol} = 0$ state if both of them coexist in the condensate. This observation matches the analysis based on scattering channels analogous to ref. 38.

3 Conclusions

In conclusion, we have observed the molecular near-dissociation levels of the photoassociated dimers produced from sodium spin-1 BEC. The spin dependent photoassociation spectra were observed, which can be used to identify good quantum numbers for some of the molecular states. The results are in agreement with theoretical predictions deduced from the analysis of ref. 38.

Author contributions

W. L., N. Z., and J. X. performed the experiments. J. W., and J. M. supervised the experimental work. V. S. contributed the theoretical analysis. All authors contributed to the analysis and discussions of the results and the preparation of the manuscript.

Conflicts of interest

There are no conflicts to declare.

Acknowledgements

This work is supported by the National Key R&D Program of China (Grant No. 2017YFA0304203), the National Natural Science Foundation of China (Grants No. 62020106014, 62175140, 61901249, 92165106, 12104276, 62011530047), PCSIRT (No. IRT-17R70), the 111 project (Grant No. D18001), the Applied Basic Research Project of Shanxi Province, China (Grant No. 201901D211191, 201901D211188), the Shanxi 1331 KSC.

Notes and references

1 M. H. Anderson, J. R. Ensher, M. R. Matthews, C. E. Wieman and E. A. Cornell, *Science*, 1995, **269**, 198.
2 K. B. Davis, M. O. Mewes, M. R. Andrews, N. J. van Druten, D. S. Durfee, D. M. Kurn and W. Ketterle, *Phys. Rev. Lett.*, 1995, **75**, 3969–3973.
3 X. Li, B. Zhu, X. He, F. Wang, M. Guo, Z.-F. Xu, S. Zhang and D. Wang, *Phys. Rev. Lett.*, 2015, **114**, 255301.
4 K. Jiménez-García, A. Invernizzi, B. Evrard, C. Frapolli, J. Dalibard and F. Gerbier, *Nat. Commun.*, 2019, **10**, 1422.
5 S. Kang, S. W. Seo, H. Takeuchi and Y. Shin, *Phys. Rev. Lett.*, 2019, **122**, 095301.
6 M. Guo, B. Zhu, B. Lu, X. Ye, F. Wang, R. Vexiau, N. Bouloufa-Maafa, G. Quéméner, O. Dulieu and D. Wang, *Phys. Rev. Lett.*, 2016, **116**, 205303.
7 K.-K. Ni, S. Ospelkaus, M. H. G. de Miranda, A. Pe'er, B. Neyenhuis, J. J. Zirbel, S. Kotochigova, P. S. Julienne, D. S. Jin and J. Ye, *Science*, 2008, **322**, 231–235.
8 T. Takekoshi, L. Reichsöllner, A. Schindewolf, J. M. Hutson, C. R. Le Sueur, O. Dulieu, F. Ferlaino, R. Grimm and H.-C. Nägerl, *Phys. Rev. Lett.*, 2014, **113**, 205301.
9 T. M. Hoang, C. S. Gerving, B. J. Land, M. Anquez, C. D. Hamley and M. S. Chapman, *Phys. Rev. Lett.*, 2013, **111**, 090403.
10 D. M. Stamper-Kurn and M. Ueda, *Rev. Mod. Phys.*, 2013, **85**, 1191–1244.
11 C. D. Hamley, C. S. Gerving, T. M. Hoang, E. M. Bookjans and M. S. Chapman, *Nat. Phys.*, 2012, **8**, 305–308.
12 Y. Kawaguchi and M. Ueda, *Phys. Rep.*, 2012, **520**, 253–381.
13 Z. Zhang and L.-M. Duan, *Phys. Rev. Lett.*, 2013, **111**, 180401.
14 C. Klempt, O. Topic, G. Gebreyesus, M. Scherer, T. Henninger, P. Hyllus, W. Ertmer, L. Santos and J. J. Arlt, *Phys. Rev. Lett.*, 2009, **103**, 195302.
15 L. S. Leslie, A. Hansen, K. C. Wright, B. M. Deutsch and N. P. Bigelow, *Phys. Rev. Lett.*, 2009, **103**, 250401.
16 E. M. Bookjans, A. Vinit and C. Raman, *Phys. Rev. Lett.*, 2011, **107**, 195306.
17 A. Lamacraft, *Phys. Rev. Lett.*, 2007, **98**, 160404.
18 J. Stenger, S. Inouye, D. M. Stamper-Kurn, H.-J. Miesner, A. P. Chikkatur and W. Ketterle, *Nature*, 1998, **396**, 345–348.
19 M. D. Barrett, J. A. Sauer and M. S. Chapman, *Phys. Rev. Lett.*, 2001, **87**, 010404.
20 T.-L. Ho, *Phys. Rev. Lett.*, 1998, **81**, 742–745.
21 T. Ohmi and K. Machida, *J. Phys. Soc. Jpn.*, 1998, **67**, 1822–1825.
22 E. Tiesinga, B. J. Verhaar and H. T. C. Stoof, *Phys. Rev. A: At., Mol., Opt. Phys.*, 1993, **47**, 4114–4122.
23 S. Inouye, M. R. Andrews, J. Stenger, H.-J. Miesner, D. M. Stamper-Kurn and W. Ketterle, *Nature*, 1998, **392**, 151–154.
24 S. L. Cornish, N. R. Claussen, J. L. Roberts, E. A. Cornell and C. E. Wieman, *Phys. Rev. Lett.*, 2000, **85**, 1795–1798.
25 J. L. Bohn and P. S. Julienne, *Phys. Rev. A: At., Mol., Opt. Phys.*, 1997, **56**, 1486–1491.
26 F. K. Fatemi, K. M. Jones and P. D. Lett, *Phys. Rev. Lett.*, 2000, **85**, 4462–4465.
27 M. Theis, G. Thalhammer, K. Winkler, M. Hellwig, G. Ruff, R. Grimm and J. H. Denschlag, *Phys. Rev. Lett.*, 2004, **93**, 123001.
28 K. M. Jones, E. Tiesinga, P. D. Lett and P. S. Julienne, *Rev. Mod. Phys.*, 2006, **78**, 483.
29 J. Stenger, S. Inouye, M. R. Andrews, H.-J. Miesner, D. M. Stamper-Kurn and W. Ketterle, *Phys. Rev. Lett.*, 1999, **82**, 2422–2425.

30 C. McKenzie, J. Hecker Denschlag, H. Häffner, A. Browaeys, L. E. E. de Araujo, F. K. Fatemi, K. M. Jones, J. E. Simsarian, D. Cho, A. Simoni, E. Tiesinga, P. S. Julienne, K. Helmerson, P. D. Lett, S. L. Rolston and W. D. Phillips, *Phys. Rev. Lett.*, 2002, **88**, 120403.
31 P. D. Lett, K. Helmerson, W. D. Phillips, L. P. Ratliff, S. L. Rolston and M. E. Wagshul, *Phys. Rev. Lett.*, 1993, **71**, 2200–2203.
32 P. A. Molenaar, P. Van der Straten and H. G. M. Heideman, *Phys. Rev. Lett.*, 1996, **77**, 1460–1463.
33 E. Tiesinga, K. M. Jones, P. D. Lett, U. Volz, C. J. Williams and P. S. Julienne, *Phys. Rev. A: At., Mol., Opt. Phys.*, 2005, **71**, 052703.
34 S. C. Bell, M. Junker, M. Jasperse, L. D. Turner, Y.-J. Lin, I. B. Spielman and R. E. Scholten, *Rev. Sci. Instrum.*, 2010, **81**, 013105.
35 S. Chu, L. Hollberg, J. E. Bjorkholm, A. Cable and A. Ashkin, *Phys. Rev. Lett.*, 1985, **55**, 48–51.
36 J. Jiang, L. Zhao, M. Webb, N. Jiang, H. Yang and Y. Liu, *Phys. Rev. A: At., Mol., Opt. Phys.*, 2013, **88**, 033620.
37 M.-S. Chang, C. D. Hamley, M. D. Barrett, J. A. Sauer, K. M. Fortier, W. Zhang, L. You and M. S. Chapman, *Phys. Rev. Lett.*, 2004, **92**, 140403.
38 C. D. Hamley, E. M. Bookjans, G. Behin-Aein, P. Ahmadi and M. S. Chapman, *Phys. Rev. A: At., Mol., Opt. Phys.*, 2009, **79**, 023401.